Naval Research Laboratory

Washington, DC 20375-5320

NRL/MR/6350--19-9885

Deformation Sensing in Soft Bio-Surrogate Materials

Christopher C. Rudolf

Multifunctional Materials Branch
Materials Science and Technology Division

May 28, 2019

REPORT DOCUMENTATION PAGE

Form Approved
OMB No. 0704-0188

1. REPORT DATE *(DD-MM-YYYY)*	**2. REPORT TYPE**	**3. DATES COVERED** *(From - To)*
28-05-2019	NRL Memorandum Report	21-02-2019 - 20-02-2019

4. TITLE AND SUBTITLE

Deformation Sensing in Soft Bio-Surrogate Materials

5a. CONTRACT NUMBER

5b. GRANT NUMBER

5c. PROGRAM ELEMENT NUMBER
NISE

6. AUTHOR(S)

Christopher C. Rudolf

5d. PROJECT NUMBER
63-N2N7-08-5

5e. TASK NUMBER

5f. WORK UNIT NUMBER
N2N7

7. PERFORMING ORGANIZATION NAME(S) AND ADDRESS(ES)

Naval Research Laboratory
4555 Overlook Avenue, SW
Washington, DC 20375-5320

8. PERFORMING ORGANIZATION REPORT NUMBER

NRL/MR/6350--19-9885

9. SPONSORING / MONITORING AGENCY NAME(S) AND ADDRESS(ES)

Naval Research Laboratory
4555 Overlook Avenue, SW
Washington, DC 20375-5320

10. SPONSOR / MONITOR'S ACRONYM(S)

NRL-NISE

11. SPONSOR / MONITOR'S REPORT NUMBER(S)

12. DISTRIBUTION / AVAILABILITY STATEMENT

DISTRIBUTION STATEMENT A: Approved for public release; distribution is unlimited.

13. SUPPLEMENTARY NOTES

Karles Fellowship

14. ABSTRACT

This report provides a detailed overview of the research findings performed to advance deformation sensing in soft materials including: 1) investigation of conductive liquids and matrix materials to enable impedance matched resistive sensors; 2) details on a custom electronics package with the necessary resolution to resolve the changes in resistance with deformation; 3) development and characterization of three rapid fabrication techniques used to generate the embedded channels for resistive, liquid metal sensors; 4) details of the gage assembly method including the encapsulation and filling of the embedded channels; and 5) experimental results from cyclic stretching of prototype soft strain sensors made using the three fabrication methods, as well as a 2-dimensional rosette-style gage and the use of conductive thread for the sensor's electrical leads.

15. SUBJECT TERMS

Soft sensors
Elastomer gages
Liquid metal gages
Channel fabrication

16. SECURITY CLASSIFICATION OF:			**17. LIMITATION OF ABSTRACT**	**18. NUMBER OF PAGES**	**19a. NAME OF RESPONSIBLE PERSON**
					Christopher C. Rudolf
a. REPORT	**b. ABSTRACT**	**c. THIS PAGE**	Unclassified Unlimited	36	**19b. TELEPHONE NUMBER** *(include area code)*
Unclassified Unlimited	Unclassified Unlimited	Unclassified Unlimited			(202) 404-1731

This page intentionally left blank.

TABLE OF CONTENTS

LIST OF FIGURES

LIST OF TABLES

This page intentionally left blank.

EXECUTIVE SUMMARY

Accurate measurement of deformations occurring within or on soft materials has recently generated interest for its benefits to the fields of soft robotics and wearable biomedical sensors. It is also currently important for bio-fidelic surrogate model testing of Personnel Protection Equipment (PPE) against blast and ballistic threats. Surrogate materials and components are tailored to mimic the response of human tissue (gels), but impedance-matched soft sensors that can measure normal and shear deformations at a point within visually-obscured elastomeric-gel materials do not currently exist. This technology gap significantly limits the value of the surrogate approach for quantifying soft tissue damage. Many proposed metrics for biological tissue damage (e.g., traumatic brain injury) employ strain (shear and normal) as parameters.

Two primary challenges in creating viable soft strain sensors are: 1) how best to measure normal and shear strains in visually obscured materials while ensuring mechanical impedance matching between the sensor and surrounding elastomeric-gel; and 2) how to fabricate and calibrate the soft sensors to operate over small to moderate to large strains (>20%) in materials that may be experiencing complex deformations at quasi-static to dynamic (wave-speed and even shock velocity) rates. The primary accomplishment of this one-year Karles Fellowship effort was the design and fabrication of rosette-style soft strain-sensor prototypes that can accurately measure three independent strains on a surface for use in calculating the components of the strain tensor (two normal and one shear component) averaged over the sensed area.

This report describes research findings generated under the Karles Fellowship award including: 1) investigation of conductive liquids and matrix materials to enable impedance matched resistive sensors; 2) details on a custom electronics package with the necessary resolution to resolve the changes in resistance with deformation; 3) development and characterization of three rapid fabrication techniques used to generate the embedded channels for resistive, liquid metal sensors; 4) details of the gage assembly method including the encapsulation and filling of the embedded channels; and 5) experimental results from cyclic stretching of prototype soft strain sensors made using the three fabrication methods as well as a 2-dimensional rosette-style gage and the use of conductive thread for the sensor's electrical leads.

The results from 1) & 2) are addressed in Chapter 2 and Appendix 1. The results from 3), 4), & 5) are addressed in detail in Chapter 3 and Appendix 2. A journal paper reporting on the fabrication techniques will be submitted for publication soon. The novel fabrication technique developed in this research (using a laser to cut flash tape on a Si wafer) is currently being used in a spin-off project looking at multi-scale surface evolution during the stretch of soft membranes. This project is in collaboration with a professor at Michigan State University and multiple journal publications are expected from this.

ACKNOWLEDGEMENTS

Christopher Rudolf was supported on this project through NRL's Karles Fellowship award.

This page intentionally left blank.

CHAPTER 1: INTRODUCTION

Deformation sensing in and on soft materials has garnered increased interest with the advancement of emerging technologies such as soft robotics, wearable computing, and biomedical applications. These applications have a need for quantification of streatching-contraction deformations along a single-axis as well as multi-directional deformation quantifications (i.e. bending, pressure, membrane stretch, planar and torsional shear). These measurement devices must conform to the movements of the device or component under test, which can be complex, involving multiple degrees-of-freedom and dynamic rates, while closely matching the mechanical properties of the system they are embedded in, such as skin, tissue, textiles, and soft actuators [1]. For example, soft actuators are increasingly used in the fields of bio-fidelic robotics and aerospace, however there is an absence of reliable positional and force feedback, which is necessary to provide a soft touch as well as accurate and controllable behavior [2]. Soft sensors are being implemented to provide this feedback, however embedding them without hindering the actuator's functionality has been a significant challenge.

Traditional strain gages, typically made of a resistive metal alloy element, cannot measure large strains (typically limited to strains < 1%). They are well suited to measure strain on stiffer materials (e.g., metals, composites, plastics), but cannot be used for strain measurements on soft materials, whose stiffness is much lower than the gage itself and whose strains may be greater than 20%, sometimes 250+%. In designing a soft strain sensor, the following requirements (application dependent) need to be considered:

1. Reliable, accurate quantification of small, intermediate, and large strains (20% +)

2. Type of quantification desired (i.e. normal or shear strain due to axial, bending, pressure, shear, or torsional loading)

3. Impedance matching of the sensor with the material system for accuracy as well as unimpeded movement

4. Biomechanically relevant strain rates and frequency responses

The objective of this research was to develop and characterize materials and sensors for measuring normal and shear strains in soft materials. Of particular interest was developing impedance matched soft strain sensors for use in anatomically-correct, bio-surrogate injury assessments in visually obscured threat protection applications.

There are three types of electromechanical, soft sensors: piezoresistive, piezoelectric [3, 4], and capacitive sensors [5-9]. Piezoresistive sensors exhibit a change of resistance under an applied deformation. The resistance change typically occurs as a result of deformation induced changes in the sensing element's physical dimensions. Piezoelectric sensors measure strain by transducing a stress-induced electric field. They are susceptible to temperature changes,

Manuscript approved April 15, 2019.

however, and flexible piezoelectric materials, such as polymers, have a low piezoelectric coefficient. Capacitive type sensors measure change in capacitance between a set or sets of embedded electrodes. Although capacitive type sensors can accommodate large deformations, they typically have very low sensitivity (gage factors < 1) [10]. For these reasons, the focus of this research was on piezoresistive type sensors.

Piezoresistive strain gages are sensors with an element that changes resistance with applied force. The applied force (displacement, pressure, bending, etc.) is converted into an electrical resistance that can be measured and correlated to displacement or strain based on the known resistivity and geometry of the gage element as well as the properties (Poisson's ratio and/or moduli values) of the system being measured. Proper selection of the gage element material is vital and the following must be considered [10]:

1. *Sensitivity and Resolution*: need to be able to discern the resistance change over the specific application range

2. *Conformability/Stretchability*: needs to conform to the expected mechanical deformations and stretch without fracturing

3. *Linearity of the Response*: nonlinearity of the response, especially as a result of large strain ranges, makes the calibration of the sensor very difficult

4. *Hysteresis*: interactions between gage element and the surrounding elastomer as well as the viscoelastic nature of soft sensor materials can result in high hysteresis

5. *Response and Recovery Time*: need to choose an appropriate material to limit the response delay

6. *Dynamic Durability*: need to account for long term, dynamic straining that accompanies many soft strain sensing applications (more important for wearable devices)

In soft sensing applications, a variety of resistive sensing elements have been investigated: conductive gels and inks [11, 12], arrays of conductive nanotubes/nanowires, ionic liquids [13, 14], aqueous solutions [15], and liquid metals [16-19].

Conductive gels and elements of nanotubes and/or nanowires are typically formed by dispersing conductive nanoparticles (i.e. carbon, graphene), nanotubes (CNTs), or nanowires (i.e. Ag, ZnO, Au) into a polymer matrix to act as the resistive sensing element. They show high sensitivity but are prone to elastic mismatch and weak interfacial adhesion resulting in poor durability. Additionally, they produce a highly nonlinear response as they undergo a change from homogenous to heterogeneous morphology due to the formation of micro-cracks upon stretching [10]. Conductive liquids, alternatively, are limited in their deformability only by the mechanical properties of the substrate that encase them. This behavior makes them a leading contender for

use in soft sensing elements where a balance of the above stated considerations is needed. For these reasons, this research focused on the use of conductive liquids for sensor element implementation.

The final issues with deploying soft sensors is how to design and fabricate the embedded liquid sensing elements and how to design and connect electronics with minimal impedance mismatch between sensing element and test lead interfaces.

In this work, three different fabrication techniques are implemented and characterized for generating resistive gage elements in soft, elastomeric sensor matrices. Cyclic uniaxial stretch experiments were performed on the gages for calculating 1D and 2D normal and shear strains. Multiple conductive liquids (ionic liquids, aqueous solutions, and liquid metals) were characterized for use as the embedded resistive sensor elements. Their reactivity, stability, sensitivity, and operating condition ranges were examined to determine the best candidate. Multiple elastomeric materials were also explored for use as the soft sensor matrix surrounding the resistive gage element. They were characterized for their ability to deform as well as their impedance matching in typical soft materials. Custom electronics were designed for providing power to and reading the response to deformation.

Report Organization

This report is organized into two main chapters. The first (Chapter 2) investigates the possible conductive liquids and sensor matrix materials as well as gives an overview of the custom electronics setups. The second (Chapter 3) describes in detail the different methods utilized to fabricate the embedded resistive element channels. An in-depth characterization of the channels is reported. The steps for assembling and filling the gages with the conductive liquid are detailed. Results of uniaxial stretch tests are reported and compared for the gages made by means of different fabrication methods. A light-weight, flexible conductive thread is implemented for connecting the gages to the electronics and a rosette-style gage of three stacked sensors is prototyped to enable 2D normal and shear strain analysis. A related journal paper comparing the fabrication techniques will be submitted for publication soon.

CHAPTER 2: METHODS: ELECTRONICS AND GAGE DESIGN

This chapter begins with an overview of the investigated conductive liquids for use as sensor elements as well as the reasoning behind the chosen liquid metal and elastomer substrate. The experimental setup, including hardware (electronics for sensor readings) configurations tested are described.

Conductive Liquid Selection

Conductive liquid embedded in an elastomer is a logical choice for making sensors to measure strains, pressures, and complex motions of soft materials that are highly stretchable and durable while maintaining a minimal impedance mismatch. The measured electrical resistivity of a liquid gage element is determined by the deformation and geometry change of the surrounding elastomer. In this research, the conductive liquids investigated were ionic liquids, aqueous solutions, and liquid metal as outlined in Table 1.

Table 1: Properties of conductive liquids

Type	Liquid	Resistivity (Ω mm)	Melting Point (°C)
Ionic Liquids	1-Ethyl-3-methylimidazolium bis(trifluoromethylsulfonyl)imide	~1,136 [1]	-17
	1-Ethyl-3-Methylimidazolium Acetate	~3571 [1]	< -20
Aqueous Solution	2.7 Mol NaCl in 1:1 vol. % of DI water and Glycerol	63.7	N/A
Liquid Metals	Eutectic-Gallium-Indium (75.5% Ga, 24.5% In by weight)	29.4×10^{-5}	15.7
	Eutectic-Gallium-Indium-Tin (68.5% Ga, 21.5% In, 10% Sn by weight)	28.9×10^{-5}	-19

[1] https://www.sigma-aldrich.com/ionicliquids. Accessed 5-July-2018

Comparative testing of the conductive liquids was performed by filling silicon tubing (Platinum-Cured Silicon Tubing, Cole-Parmer) with inner diameter of 0.012". Tube lengths of 100 mm were filled with the respective liquids, 30 gage Copper wire was inserted into each end, and a silicon sealant (Silpoxy, Smooth-On) was used to encapsulate the ends. The use of ionic liquids generated starting resistances on the order of $1.5 \times 10^6 – 5 \times 10^6$ Ω. The ionic liquids initially resulted in operable sensors but as time went on (days later), subsequent testing showed drastically different resistance values. This was determined to be the result of a reaction between the copper test leads and the ionic liquids. This instability and the toxicity of the ionic liquids deemed them a poor choice. The aqueous solution of sodium chloride mixed with 1:1 vol. % DI water and glycerol resulted in a starting resistance of ~87,000 Ω. The addition of glycerol provided greater viscosity to the solution which better matched the impedance of the surrounding elastomer matrix. The initially operable sensors, however, lost continuity after a few days as both air bubbles and precipitates of NaCl crystals formed in the tube. Chossat et al. [13] previously

reported that above 1.23 volts, electrolysis of water divides molecules to produce hydrogen and oxygen which renders the sensor non-functional. Liquid metals have garnered interest as they are flexible and can provide a functional element over any range of stretch that the surrounding elastomer matrix can attain. Both eutectic-GaIn and eutectic-GaInSn (Galinstan) have similar conductivity properties, however the addition of Sn reduces the melting point from 15.7 to -19 °C. For the purposes of this research, eutectic-GaIn (Solution Materials, Santa Clara, CA) was chosen for its availability and low cost. The ionic liquid resulted in an initial resistance of 0.40 Ω when filled in the 100 mm length of silicon tubing. While many think that liquid metals are toxic (as a result of liquid metals being associated with Mercury), e-GaIn has low toxicity. Unlike the other liquids tested, the e-GaIn test sensor showed long-term stability over time.

Gage Design – Sensor Matrix Material

The primary factors in choosing an elastomer for embedding a liquid metal element are ability to stretch and deform without fracture and hardness for impedance matching to the application. Previous research has utilized elastomers, the most common of which are Polydimethylsiloxane (PDMS) and platinum-cure silicones to make up the bodies of the soft sensors. The typical properties are listed in Table 2.

Material	Material Class	Elongation at break	Tensile Strength (MPa)	Shore Hardness	Working Time (minutes)
Sylgard 184 [1]	PDMS	~160 % [2]	6.7	43	90
Smooth-Sil 950 [3]	Platinum-Cure Silicone	320 %	2.17	50A	45
EcoFlex 00-30 [4]	Platinum-Cure Silicone	900 %	1.38	00-30	45

[1] https://consumer.dow.com/content/dam/dcc/documents/en-us/productdatasheet/11/11-31/11-3184-sylgard-184-elastomer.pdf?iframe=true. Accessed 4-April-2019

[2] Case et al. Soft Robotics 2015, Vol. 2, Number 2, pages 80-87.

[3] https://www.smooth-on.com/products/smooth-sil-950/. Accessed 4-April-2019

[4] https://www.smooth-on.com/products/ecoflex-00-30/. Accessed 4-April-2019

Based on the properties, mainly the elongation and ability to conform due to its soft nature, EcoFlex 00-30 (Smooth-On, Inc., Macungie, PA) was chosen as the elastomer for the gage matrix. Sil-Poxy (Smooth-On Inc.), a single component adhesive for bonding platinum-cure silicone to itself and other objects, was purchased to seal the liquid metal gage-elements where they interfaced with the test leads.

Experimental Setup and Electronics

Traditional metal foil strain gages have a standard, calibrated resistance on the order of 120 or 350 Ω, and can be easily implemented using ready-made conditioning circuits. Custom soft

sensor modules made with liquid metal elements tend to have much smaller resistance values, on the order of 1 – 10 Ω. The low resistance value amplifies the error possibilities resulting from signal noise and lead wire connections. The initial experimental setup utilized a DC power supply and decade resistance boxes to complete a Wheatstone bridge circuit. This method, while more accurate than just attaching a multimeter, had considerable error due to the compounding errors of the resistance boxes.

A custom-built breadboard (Figure 1) was designed and assembled. A fixed current (0.1 Amps) was supplied to the sensor by converting the output 3.3 volts from the Arduino Leonardo microcontroller board through a potentiostat, an operational amplifier (LTC1052, Linear Technology), and a power MOSFET (IRF510, Vishay Siliconix). A differential of the gage voltage was read using a 16 bit analog-to-digital converter (ADC) with programmable gain (ADS1115, Texas Instruments) for amplifying the read voltages. The output of the ADC was connected with the Arduino microcontroller which interfaced via USB to a computer running Matlab. The voltage was logged and converted to resistance via the Matlab program.

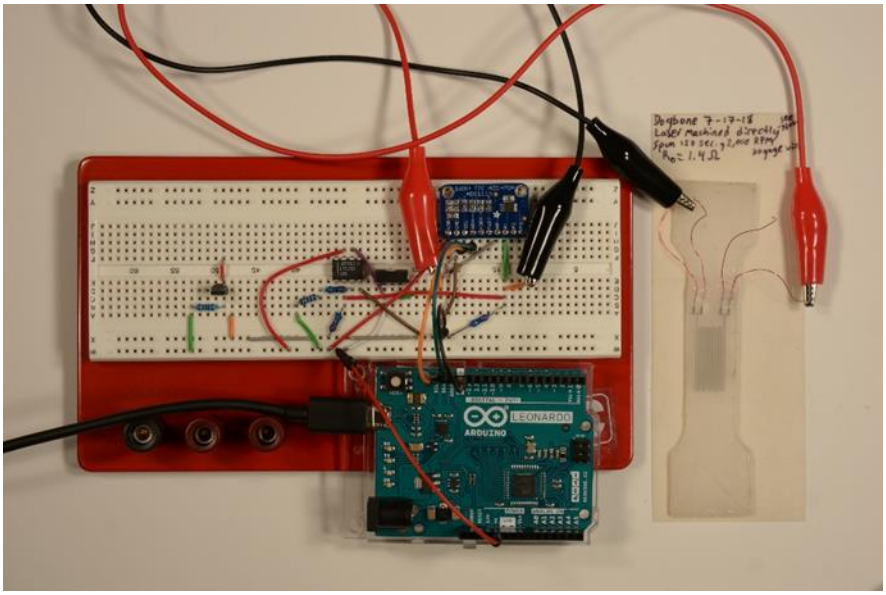

Figure 1: Image of the custom-built breadboard setup used to supply constant current to the sensor, condition and amplify the signal, and interface with a computer for data logging and plotting.

This custom electronics package provided readings with the resolution necessary for the gages being built. The benefit of this custom setup is that it is inexpensive and can be made into a small form factor, non-breadboard system-on-chip for implementing and controlling the gage in small spaces with low power consumption. The nature of the temporary connections in the breadboard setup showed problems with reproducibility due to vibration and poor connections.

A final lab-scale electronics setup utilized a National Instruments (NI) data acquisition (DAQ) system with a custom Labview code. A NI PxIE-4139 high-precision source measure unit was programmed via the Labview code to supply a constant current of 0.1 Amps to the sensor(s). The

setup was wired for up to 3 sensors in series but is expandable up to 8. Kelvin clips (silver insulated, Mueller Electric Company) were utilized to connect to the sensor leads thereby removing the lead wire resistance from affecting the measured readings by supplying current and reading voltage separately. The voltage readings were converted from analog to digital signals through an NI PxIE-6361 DAQ module and converted to resistance values in the Labview code. This setup had the additional benefit of interfacing with a non-contact video extensometer (MTS AVX) for accurate displacement and strain measurements during testing. The AVX was controlled by a dedicated laptop running MTS Video Extensometer software. It stored video captured during testing and provided four real-time analog outputs (three strains and time) that were read by the NI DAQ/Labview system. The AVX analog outputs were ± 10 volt signals with signal-to-voltage calibration set in the Labview software. Additional information can be found in Appendix 1.

CHAPTER 3: GAGE FABRICATION TECHNIQUES AND RESULTS

Techniques for fabricating elastomer gages with embedded serpentine channels for liquid-metal elements include syringe printing [11, 12], freeze casting [20], photolithography [21], 3D printing of molds [16, 17, 22], direct laser ablation of an elastomer substrate [23], and laser rastering a mold from acrylic [13]. Direct-write of the channels via syringe printing has the benefit of not requiring a mold, however specialized, custom-built tools are required and the syringe tip has a tendency to clog due to surface oxides of the liquid metals. Freeze casting is a novel technique that takes advantage of the melting point of the liquid-metal (MP of e-GaIn = -19 °C), however it has the limitation of creating simple geometries that are on the order of 0.5 mm widths and larger. Photolithography is the most-used method for creating molds with the smallest channels (< 100 μm widths) but requires photomasks and a very clean environment for assembly. This research focused on making elastomeric sensors on the mm length scale with the smallest channel dimensions = ~100 μm. Advances in 3D printing have enabled these length scales to be obtained using inexpensive fused deposition 3D printers. Unfortunately an acquisition delay resulted in the purchased 3D printer to arrive much later than expected and therefore this research evaluated 3 different methods: 3D printing, direct laser-patterning, and laser cutting flash tape.

This chapter begins with detailed descriptions of 3 different fabrication methods utilized in this research. The sensor assembly and filling steps are described and a thorough characterization of dogbone-shaped gages and their embedded channels is detailed. Uniaxial 1-D stress-strain analysis was performed and the results are compared. This chapter finishes with a description and uniaxial tensile characterization of a three-sensor rosette-style gage with sensors aligned with 0, 45 and 90 degrees for full 2D strain characterization.

Gage Channel Fabrication Techniques

3D Printing

With advances in additive manufacturing (3D printing), molds for casting elastomer sensor bodies with serpentine channels can be designed and printed inexpensively. The purchased fused deposition (FDM) printer (Prusa I3 MK3S, Prusa Research) with 0.25 mm extruder nozzle had a layer height resolution of 50 μm and superior x-y resolution (value dependent on print speed and other factors) than other FDM printers currently on the market. Since this printer was delayed, molds were made with two other FDM printers: the Makerbot Replicator 2 (Makerbot/Stratasys, Brooklyn, NY) and Makergear M2 (Makergear, Beachwood, OH). Both printers were unable to achieve printed molds with the designed channel width, spacing, and height. An EOS P396 (EOS GmbH, Munich, Germany) selective laser sintering printer using PA 2200 polyamide 12 powder was used to make molds for testing and characterization. The printer had a set layer height of 100 μm. Initial rectangular shaped molds (36 x 45 mm) with 6 serpentine channels of 20 mm length (Figure 2) and differing prescribed geometries (Table 2) were printed and evaluated for accuracy.

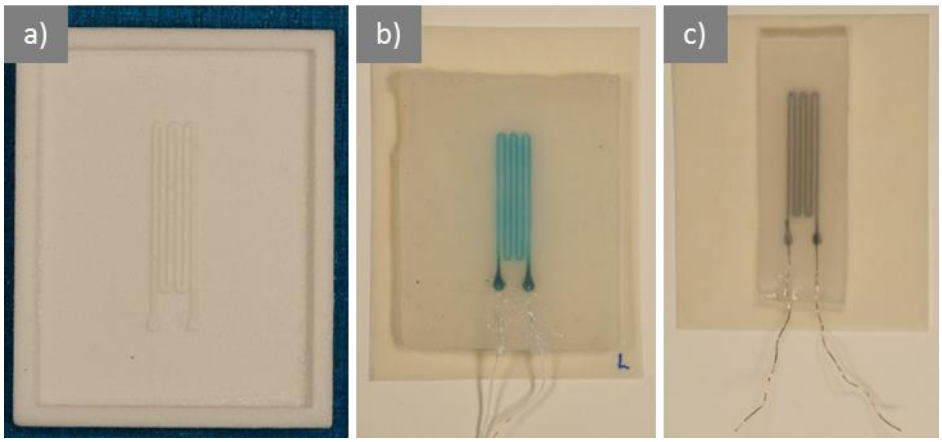

Figure 2: Photos of a) initial rectangular mold with serpentine channels printed using the EOS P396 selectrive laser sintering printer, b) assembled gage with channels filled with a blue food coloring added aqueous solution, and c) an assembled gage filled with eutectic-Gallium-Indium liquid metal.

Table 2: Initial EOS P396 rectangular mold accuracy evaluation.

Part #	Prescribed Width (mm)	Prescribed Height (mm)	Actual Width (mm)	Actual Height (mm)
Part 1	0.3	0.3	0.440 – 0.460	0.300 – 0.400
Part 2	0.3	0.2	0.430 – 0.460	0.220 – 0.248
Part 3	0.2	0.2	0.440 – 0.460	0.272 – 0.275

The measured widths and heights were found using a Keyence VHX-6000 digital microscope and the range of measurements found from 10 points is reported.

A final dogbone shaped mold (Figure 3) was designed with 20 channels of prescribed heights, widths, and spacing of 0.15, 0.3, and 0.4 mm, respectively with lengths of 20 mm each. The fill ports where the test leads are inserted are designed to be 2 mm in length by 0.8 mm in width. The channels of this mold (including turns and fill ports) have a prescribed volume of 19.91 mm^3 (~0.02 mL).

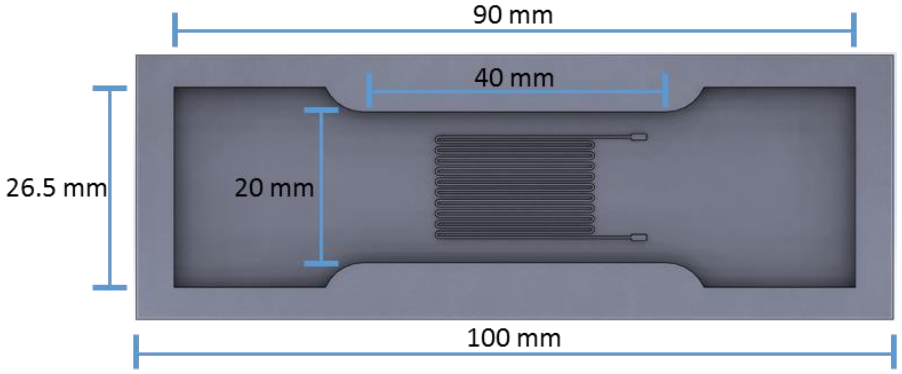

Figure 3: Final dogbone shaped sensor mold.

Direct-Laser Patterning

The technique of laser patterning utilized a 50 watt CO2 laser (Epilog Legend Mini 24, Epilog Laser, Golden, CO) and was used for two fabrication techniques. The first technique used laser

rastering on a piece of acrylic to generate a mold for casting with an elastomer (Figure 4a). This method was very much a trial-and-error approach that was time-intensive and took many passes to produce this mold with a depth of 1.37 mm and a channel height and width of 0.61 and 0.56 mm. The difficulty in controlling the prescribed heights and the resulting textured substrate negated the eventual use of this method.

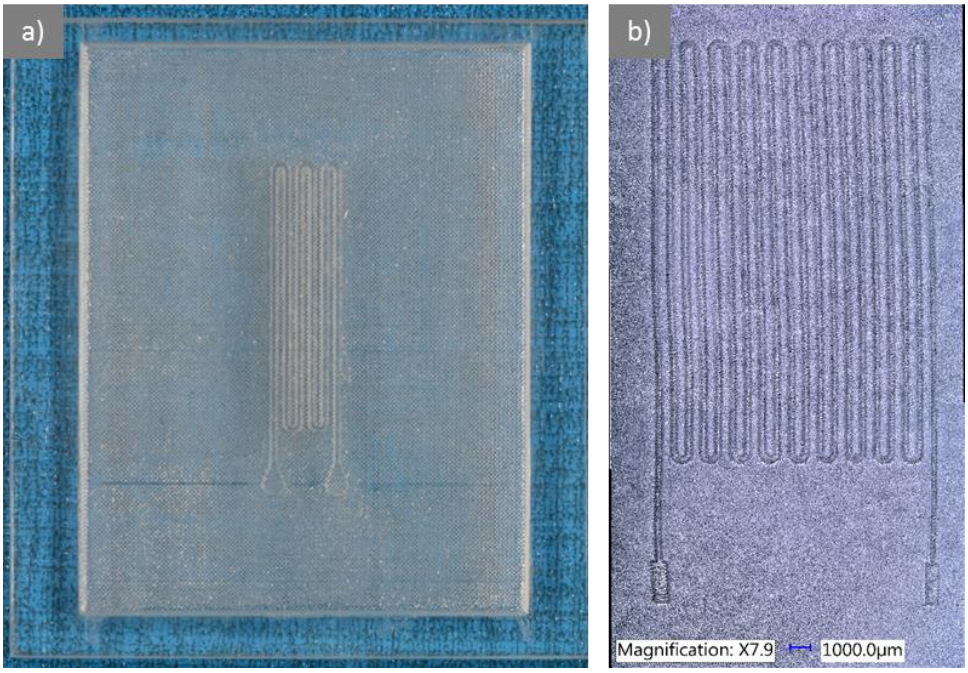

Figure 4: Photo of a) rectangular test mold fabricated by laser rastering on acrylic and b) serpentine channels directly laser rastered on already cured EcoFlex 00-30.

The second method that utilized direct-laser patterning involved direct rastering on already cast and cured EcoFlex 00-30 elastomer (Figure 4b). Different channel width and spacing combinations were attempted and different combinations of laser power, speed, and dithering type were evaluated. Final prescribed channel widths of 0.3 mm width and 0.4 mm spacing were fabricated with laser settings of 80% power, 50% speed, 1200 dpi, and standard dithering. The channels and surrounding area were cleaned with IPA by wiping with cotton swabs and kim-wipes to remove the ablated material residue.

Laser Cutting of Flash Tape

The final channel fabrication technique was a novel idea that has not been previously reported in literature at the time of fabrication. In order to achieve uniform channel height, flash tape of 0.15 mm thickness was adhered to a piece of acrylic before being vector cut using the same Epilog CO2 laser. It was determined that the laser settings needed to fully cut through the tape also resulted in the acrylic substrate being partially cut, making the channel mold inoperable as the heights were no longer uniform. To address this issue, flash tape was adhered to polished Si wafers (100 mm in diameter), allowing the flash tape to be cut while the reflectivity of the wafer

did not allow any engraving of the substrate to occur. The width of the channels was prescribed to be the same as the other two methods (0.3 mm). After trying many different laser settings and measuring the results, the optimal parameters were determined to be 9% power, 40% speed, 1200 dpi, and 5000 Hz frequency vector cuts. Figure 5 shows the fabrication steps: a) as cut laser channels on the Si wafer substrate, b) and c) the removal of surrounding tape, d) the prescribed serpentine channel pattern that is left on the Si substrate, and e-f) the placement of an acrylic mold to be filled with EcoFlex 00-30 silicone to make the channel side of a soft gage. When casting of the mold with channels was done by clamping the desired acrylic mold shape directing onto the Si wafer. Applying mold release (Ease Release 200, Smooth-On, Macungie, PA) 5 minutes prior to casting allowed the cured silicone elastomer to be removed without pulling up the tape. This enabled these patterns to be used multiple times (up to ~10) before eventual delamination.

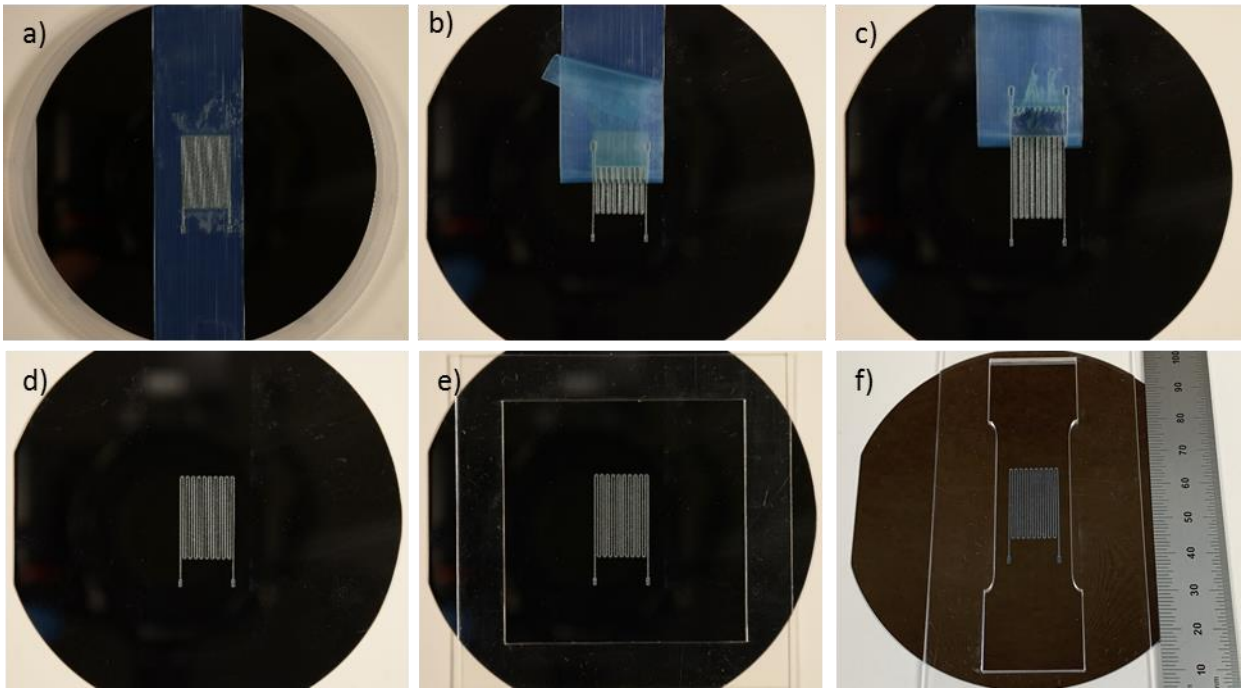

Figure 5: Photos of the process of laser cutting flash tape on a silicone substrate to be used as a mold for casting a soft serpentine channel sensor.

Gage Assembly Method

The assembly method for all three gage types was the same. The process involved casting and curing an elastomer layer without channels, spin-coating a thin layer of the same elastomer, and bonding the cured layer with channels together with the layer without channels to encapsulate them. A dogbone-shaped (or rectangular as shown in Figure 5e, depending on gage being assembled) mold for casting the solid encapsulation layer was formed by laser cutting a 1.66 mm thick piece of acrylic that was then adhered to solid acrylic using 3M double sided tape (tape thickness of 0.16 mm). Two-part EcoFlex 00-30 was combined 1:1 (vol. or weight) and stir-mixed for 3 minutes. It was placed in a vacuum chamber and degassed until no bubbles remained (typically 5-10 minutes). The degassed EcoFlex was poured into the mold, covered with a

smooth acrylic sheet and weighed down to ensure accurate, reproducible thickness between gages. Once cured (4 hours), the layer without channels was adhered to a solid piece of acrylic using double-sided flash tape and uncured EcoFlex was applied as shown in Figure 6a. The EcoFlex was first evenly spread over to cover the entire layer before being spin coated for 4 minutes at 2,000 RPM. The spin-coated layer (~ 10-15 μm thick) was allowed to sit at room temperature for 20 minutes to allow for a tacky consistency before the top layer with channels was gently applied (ensuring no air bubbles) to the unpatterned layer to encapsulate the channels (Figure 6b). Assembling when the adhesion layer reached a tacky consistency reduced the chance of flow into the channels during bonding. A layer of EcoFlex was applied to the surrounding edges (Figure 6c) for added adhesion. Once cured, the assembled gage was removed from the backing and was ready for filling of the channels.

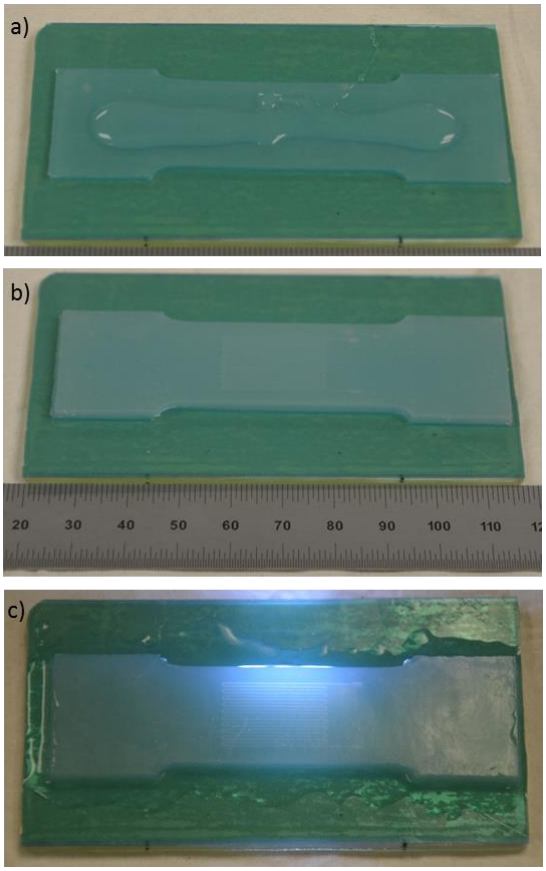

Figure 6: Photos of the gage layer assembly process: a) uncured EcoFlex 00-30 is poured into the cured layer without channels, b) after spin-coating the layer with channels is adhered to the solid layer, and c) extra EcoFlex is lapped around the assembled gage for added adhesion.

Filling of the encapsulated channels was achieved using two 1 cc manual syringes fitted with 27 gauge needle tips. An empty syringe first inserted into one of the fill ports. The other syringe was filled with ~0.2 mL of e-GaIn and inserted into the other fill port (Figure 7). As the e-GaIn syringe was depressed, the empty syringe was used to remove the entrapped air. Once filled, the syringes were removed and 30 gage magnetic copper wire (35 mm in length with 5 mm of insulating coating stripped from each end by soldering iron) was inserted into the fill ports following the pathways left by the syringes. Small amounts of SilPoxy silicone adhesive (Smooth-On Inc.) was applied to seal the interface of the lead wires and channels.

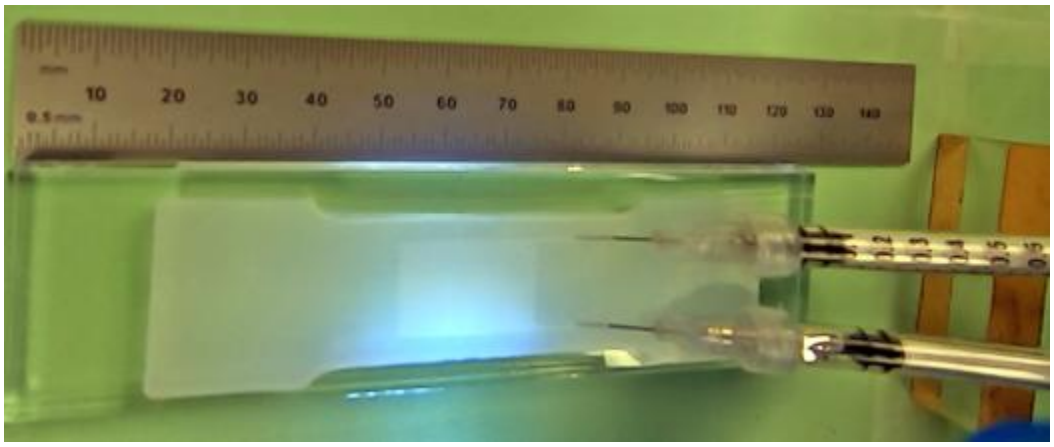

Figure 7: Photo of process for filling embedded channels with liquid metal.

Characterization of Channel Geometry

The embedded channels are characterized using a Keyence VHX-6000 digital microscope by imaging and measuring the channels prior to gage assembly and filling. The microcope performed 3D image stitching to capture height data across the channels and allowed the quantification of channel geometry.

3D Printed Channels

The channels formed after casting the printed mold are shown in Figure 8. The channels have rough edges as a result of the printing process that sinters powder particles together. Additionally, the roughness of the molds created a textured surface, whereas the other two methods had a smooth surface to be bonded to the encapsulating, solid side. This is evident in Figure 8e. The channels created via this fabrication technique were the most uniform (Figure 9), having the least tapered channel sidewalls compared to the other two methods. The average channel cross-sectional area was 0.1235 mm^2 which is ~ 2.7 times the prescribed cross-sectional area. This difference was the result of the resolution of this 3D printing process. The calculated theoretical initial resistance (Equations 1 and 2) for these gages is 1.047 Ω

$$R_{theoretical} = \rho \frac{L_0}{A_0} \quad \text{…. Equation 1}$$

$$A_0 = h_0 \frac{a+b}{2} \quad \text{…… Equation 2}$$

where ρ is the resistivity of e-GaIn, L_0 is the initial total channel length and the cross-sectional area is taken as a trapezoid where a and b are the top and bottom widths, respectively.

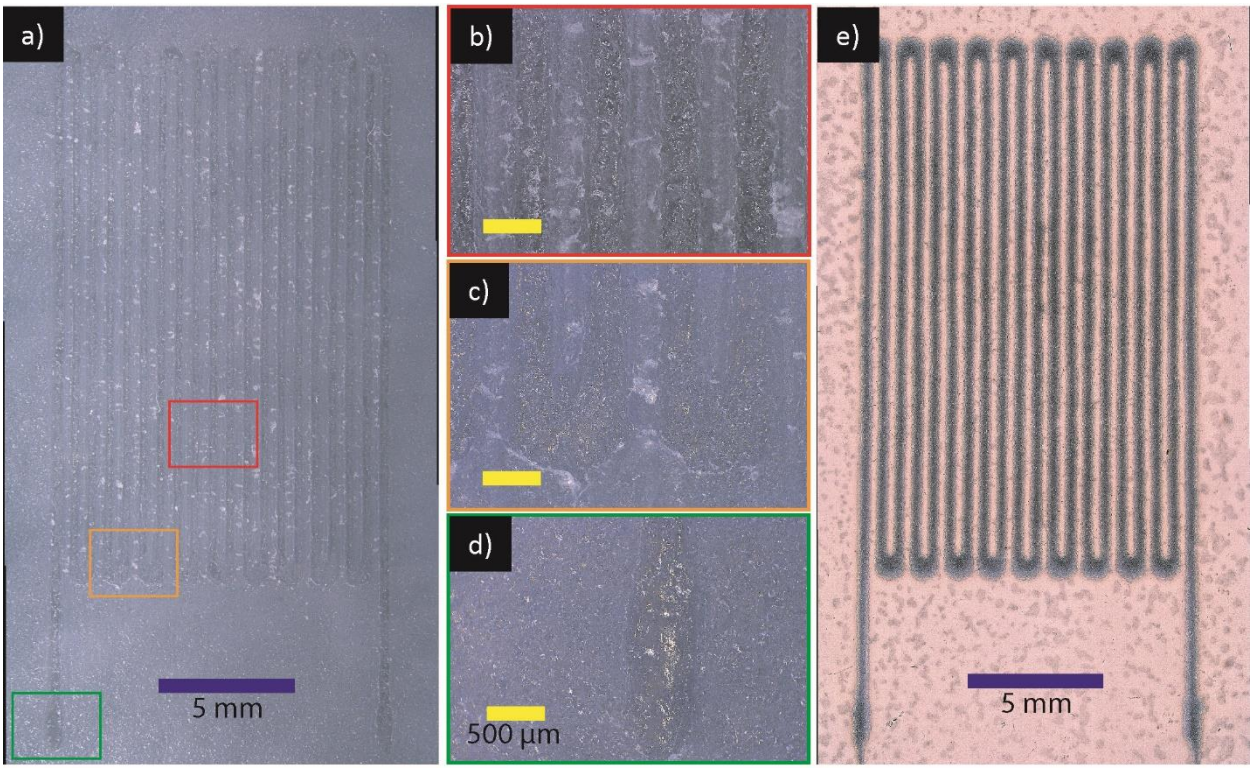

Figure 8: Images taken via digital microscope of the channels formed when cast with the 3D printed mold: a) stitched image showing entire gage area, b-d) magnified views as marked on (a) of the channels, turns, and fill ports, respectively, and e) stitched image showing the fully assembled and filled gage.

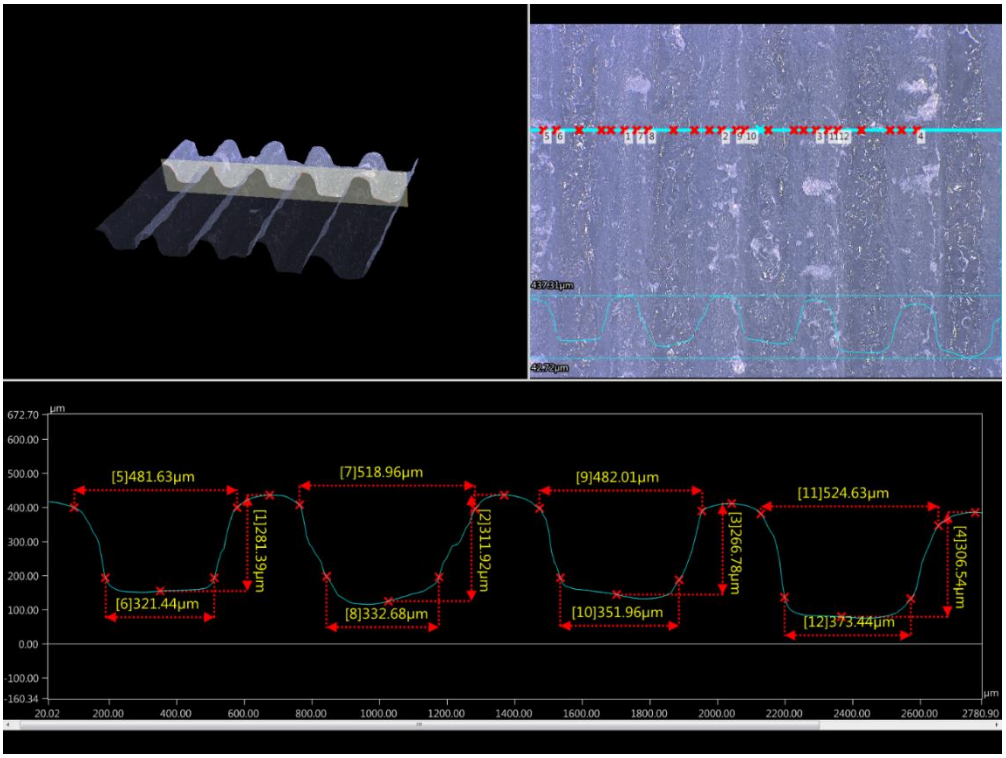

Figure 9: Channel measurements and morphology taken via the Keyence digital microscope for channels formed when cast into the 3D printed mold.

The reproducibility between castings is excellent with minimal variations observed. The discrepancy between the prescribed and measured actual channel geometries is expected to be considerably, if not entirely, reduced had we fabricated the mold using the desired 3D printer that was delayed. Additionally, the surface and channel finish would be considerably smoother using a FDM printing method. Nevertheless, these gages are viable, working gages with the necessary stretch ability for soft sensors.

Direct Laser Patterned Channels

The channels formed via direct laser ablation are shown in Figure 10. The channels have a dithering texture as a result of the horizontal raster of the laser. The spacing between and area surrounding the channels maintained their smooth surface, enabling a strong bond when encapsulating the channels with the solid layer. The smooth bonding area also provided greater transparency through the assembled sensor compared with the 3D printed mold cast, as evident in Figure 10e. The channels created via this fabrication technique had a tapered channel geometry (Figure 11) that fell between the other two methods. The average channel cross-sectional area was 0.054 mm^2 which is only 1.2 times the prescribed cross-sectional area. This difference could be less in future gages by reducing the laser power or increasing the raster speed. The calculated theoretical initial resistance for these gages is 2.406 Ω.

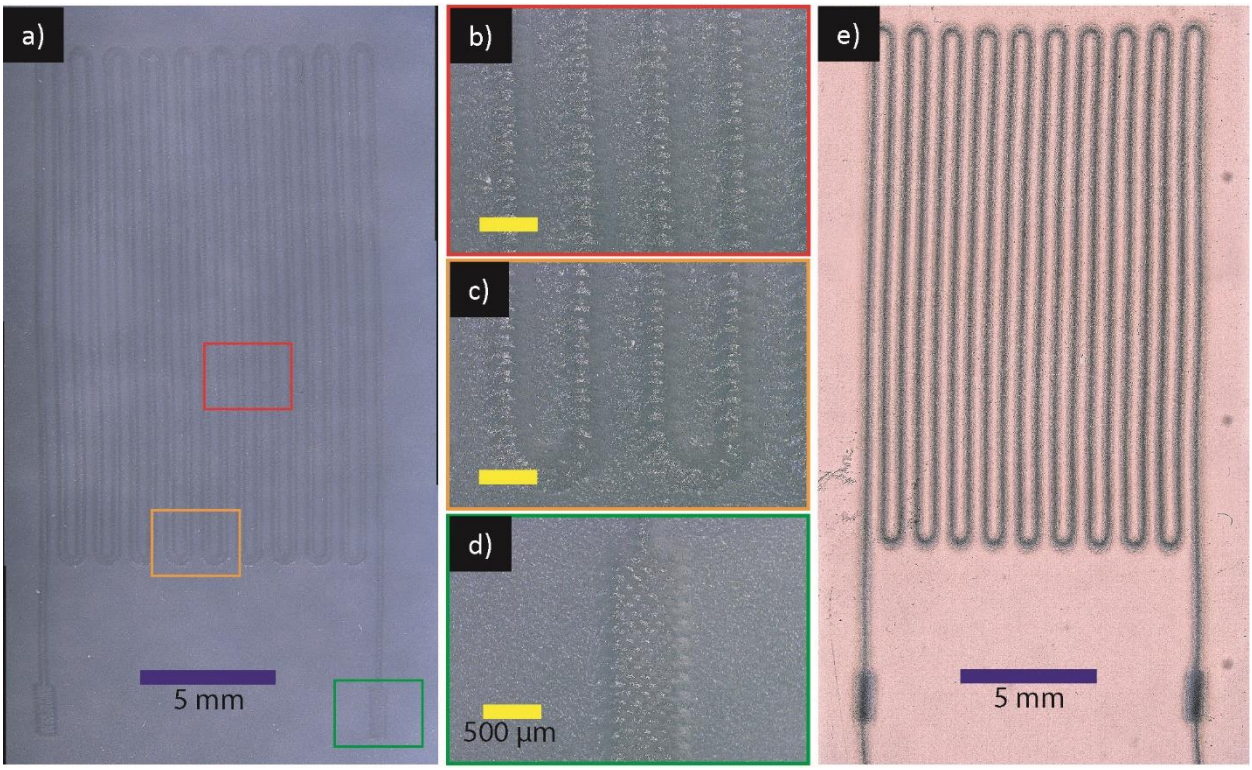

Figure 10: Images taken via digital microscope of the channels formed by direct laser raster fabrication: a) stitched image showing entire gage area, b-d) magnified views as marked on (a) of the channels, turns, and fill ports, respectively, and e) stitched image showing the fully assembled and filled gage.

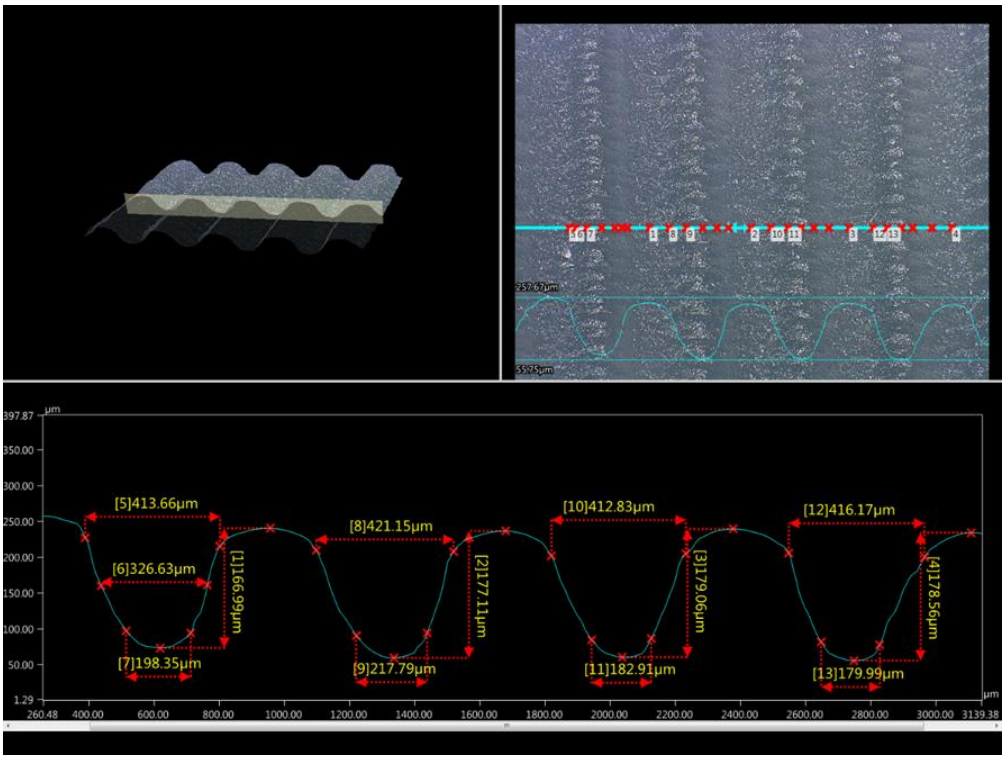

Figure 11: Channel measurements and morphology taken via the Keyence digital microscope for channels formed via direct laser raster.

The direct laser ablation technique proved to be a very quick process that could be used for making complex patterns with ease. The minimum channel geometry of this method is only limited by the emitted wavelength of the laser module (10.6 µm) and raster style.

Laser-Cut Flash Tape Channels

Channels formed by casting EcoFlex onto tape laser cut on a Si wafer are shown in Figure 12. During the laser vector cutting, the tape heats up and melts preferentially towards the top, resulting in a rounded trapezoidal channel geometry (Figure 13). This method generated channel edges that were well defined with the greatest alignment compared with the other two fabrication methods. Casting on the smooth Si wafer provided a very smooth surface between and around the channels, enabling a strong bond with the encapsulating layer during assembly. As was the case with the direct laser ablation method, these sensors had better transparency due to the smooth surface (Figure 12e). The average cross-sectional area for the channels was 0.041 mm^2 which is just below the prescribed channel cross section. The reduction in width as a result of melting during laser cutting is the reason for this. The channel height averaged 0.184 mm found to have been caused by melted buildup and slight bubbling in the tape during laser cutting. The theoretical initial resistance based on the channel dimensions for these gages is 2.834 Ω.

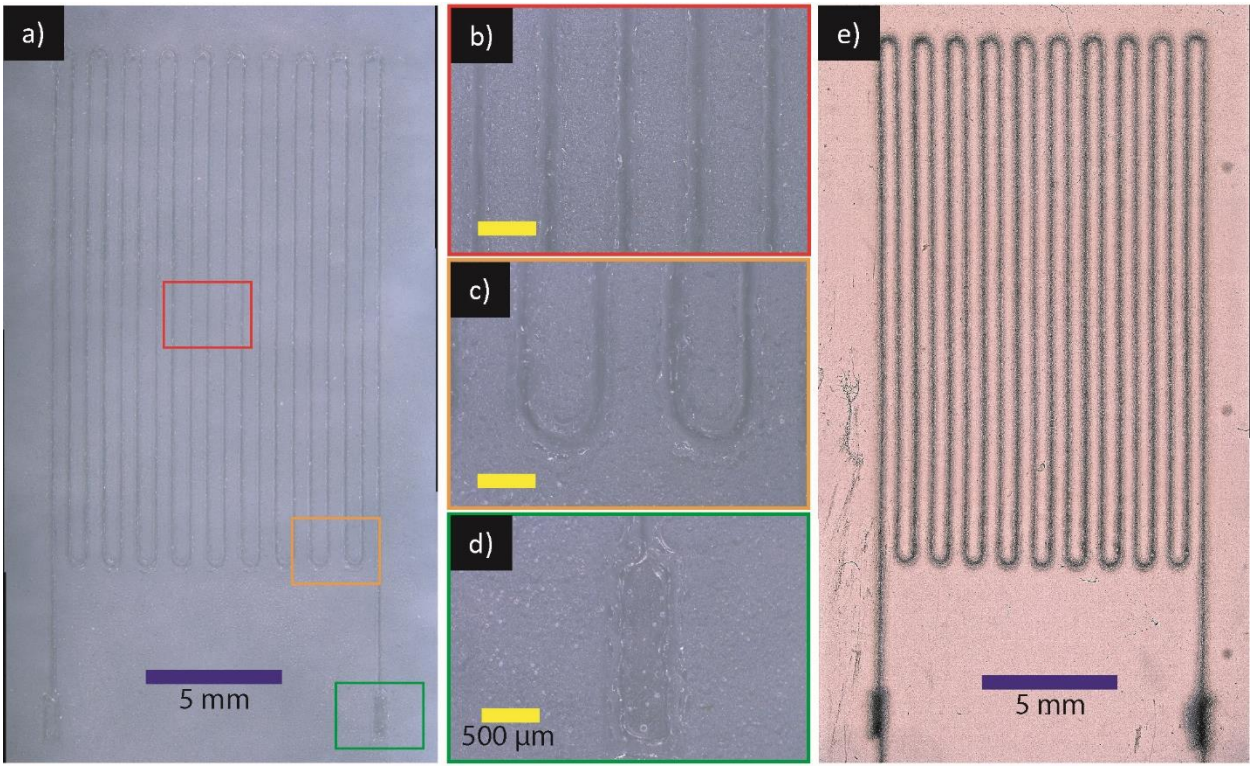

Figure 12: Images taken via digital microscope of the channels formed when cast onto laser cut flash tape: a) stitched image showing entire gage area, b-d) magnified views as marked on (a) of the channels, turns, and fill ports, respectively, and e) stitched image showing the fully assembled and filled gage.

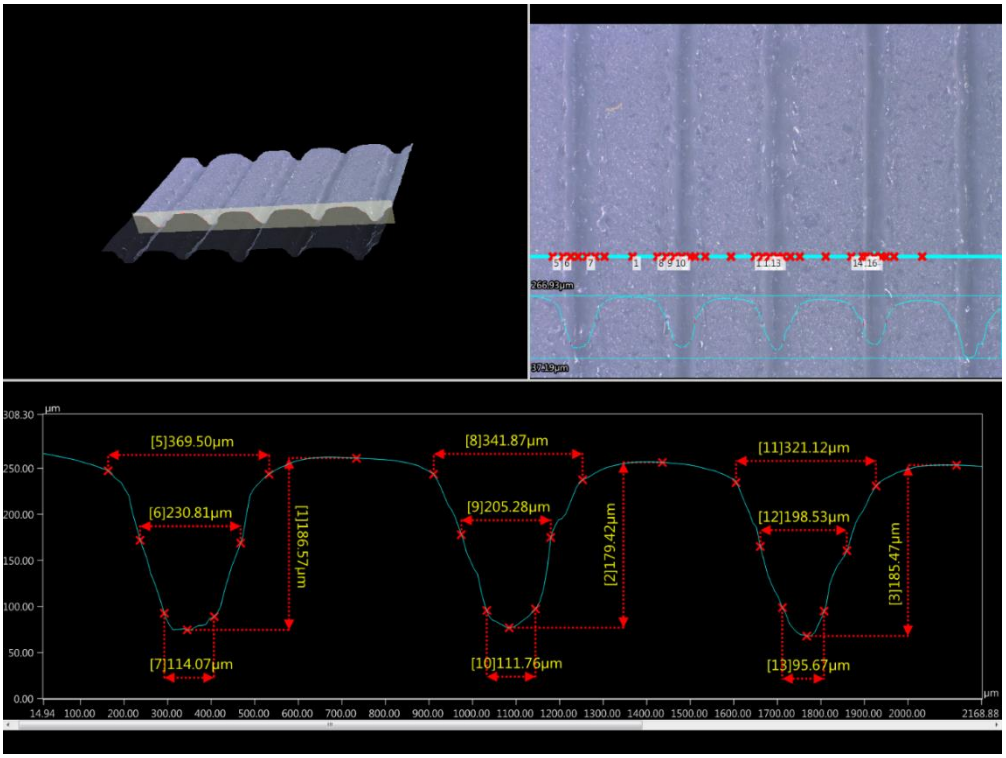

Figure 13: Channel measurements and morphology taken via the Keyence digital microscope for channels formed when cast onto laser cut flash tape.

Uniaxial, Cyclic Stretching - Results and Discussion

Three dogbone shaped gages of each fabrication technique were assembled and tested via uniaxial tension using an ElectroPuls E3000 laboratory materials test system (Instron Corp., Norwood, MA). Cyclic uniaxial stretching (5 cycles) from 0 to ~50% strain was performed at a rate of 1 mm/sec. The axial and transverse strains were recorded via the AVX by tracking the edges of the liquid metal in the gage. The custom Labview program and NI PxIE system set and supplied the constant current of 0.1 Amps and read the voltage change across each gage during testing. The resistance and normalized gage sensitivity (Equation 3) were calculated and logged in sync with the strain readings.

$$Gage\ Sensitivity = \frac{R-R_0}{R_0} = \frac{\Delta R}{R_0} \quad \text{..... Equation 3}$$

$$Gage\ Factor = \frac{(\Delta R/R_0)}{\varepsilon} \quad \text{..... Equation 4}$$

In this section, the soft sensors are characterized in terms of the performance parameters listed in Chapter 1: *sensitivity, conformability/stretchability, linearity, and hysteresis*. The normalized sensitivity versus strain results are compared (Figure 14) and the gage factors (Equation 4) are calculated for each of the tested gages. The gage factors reported are found by linear fit of the sensitivity – strain plots.

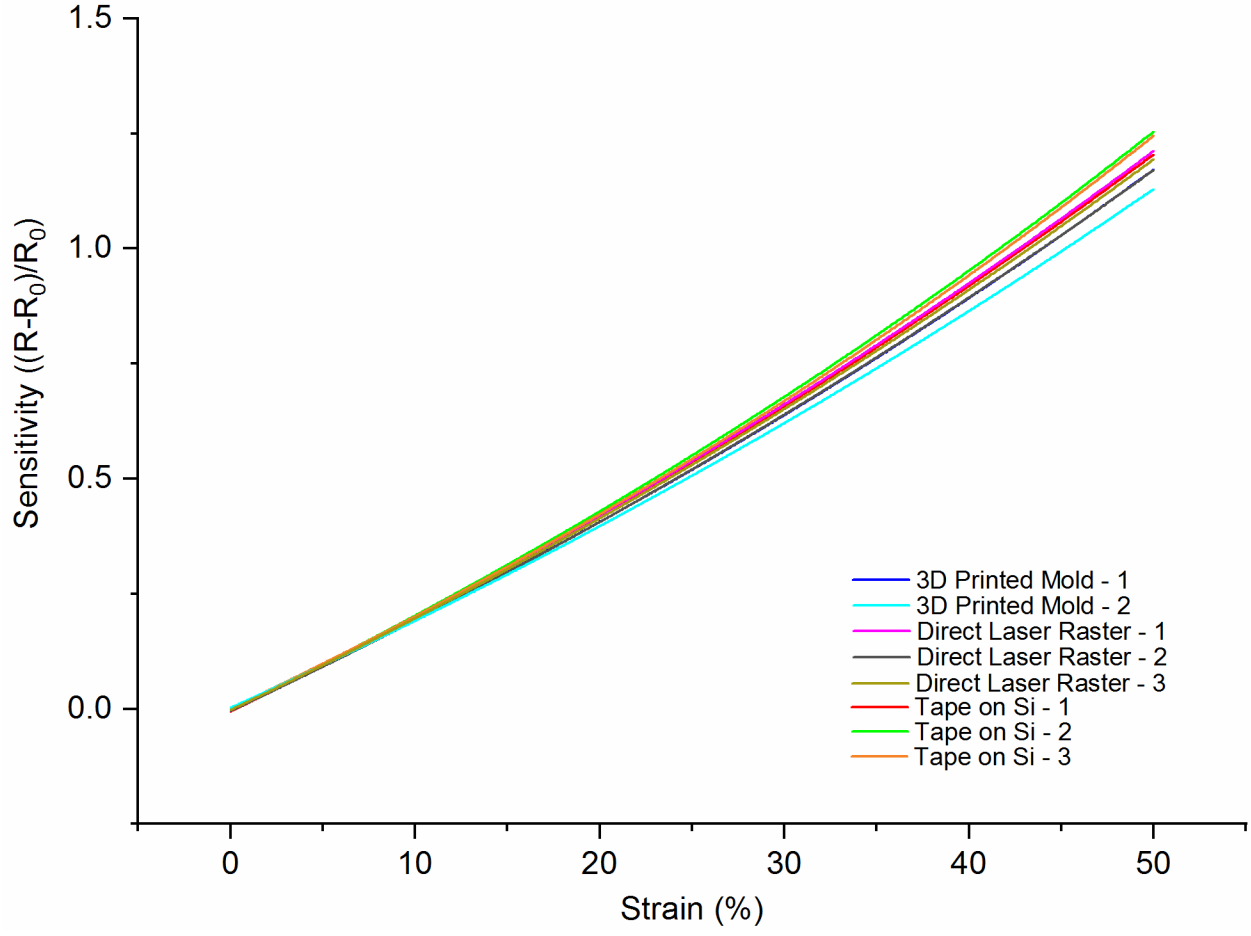

Figure 14: Sensitivity versus strain plots of the uniaxial tensile stretch tests.

A summary of the experimental results is found in Table 3. The e-GaIn volume was found by weighing the gage before and after injecting the liquid metal and dividing by the density of the e-GaIn (6.25 g/mL). Unfortunately, 3 gages were assembled before this weight method was enacted. The manual syringe method of filling the channels with liquid metal resulted in poor reducibility. For the same channel fabrication techniques, and thereby near-identical channel geometry, the amount of liquid metal injected can vary significantly. This results from the soft surrounding silicone elastomer matrix which can easily expand when a fluid is injected. The initial resistance of the gage was dependent on the amount of liquid metal injected. For greater reproducibility, automatic syringe pumps could be used.

Table 3: Experimental result summary from uniaxial tensile stretch testing.

Gage	e-GaIn Volume (mL)	R_0 (Ohms)	Gage Factor (linear fit)
3D Printed mold – 1	0.0576	1.0550	2.3142
3D Printed mold – 2	0.0528	1.0700	2.3008
Direct Laser Raster – 1	N/A	1.1430	2.4265
Direct Laser Raster – 2	0.0400	1.2840	2.3513
Direct Laser Raster – 3	0.0320	1.5880	2.3744
Tape on Si – 1	N/A	1.6230	2.4591
Tape on Si – 2	N/A	1.9300	2.5305
Tape on Si – 3	0.0240	2.4210	2.4934

The sensitivity of a strain gage is typically given by the gage factor. For the fabrication techniques tested, the average gage factors were 2.3075, 2.3841, and 2.4943 for the 3D printed mold, direct laser raster, and tape on Si methods, respectively. These gage factors indicate that any of the fabrication techniques can be used to make sensors that can discern a resistance change with respect to stretch in this range. The stretchability of all three gage types was the same as the only difference between the gages was how the channels were fabricated. The stretchability is more dependent on the elastomer material for the surrounding matrix.

Linearity is extremely important over the expected strain range (application specific). Any non-linearity in the resistance response would make calculating the calibration of the sensor complex. All tested gages had a near-linear response (Figure 14) and could be accurately calibrated using a theoretical linear fit. No hysteresis was detected in any of the gages over the range and rate tested. See Appendix 2 for the plots of resistance change with strain over multiple cycles. This was expected as the liquid metal is homogeneous, whereas hysteresis is typically observed in soft gages with resistive elements made of non-homogeneous particles or platelets that can rapidly deform in one direction but take longer to reset.

Conductive Thread as Test Leads

One of the challenges associated with soft elastomeric sensors is the impedance mismatch at the interface between the soft liquid metal sensor element and the copper wire test leads. To combat this issue, conductive thread (Liberator 40, Syscom Advanced Materials, Columbus, OH) was tested as the lead wire (Figure 15). The thread is composed of a high-strength Vectran fiber core with a conductive metal outer layer. It is 72% lighter than the 30 gage copper wire used in the other gages with 5 times the break strength. Composed of 40 filaments that are twisted at 4.5 twists/inch, the thread provided a flexible electrical path that won't impede the gage's ability to conform to complex movements. A gage with channels fabricated by casting tape on Si wafer

was assembled in the same manner as the other gages, however instead of inserting copper wires, the conductive thread was used. Inserting the thread was in itself a challenge. Unlike the copper wire which is stiff enough to follow the paths left by the syringes, the thread is light-weight and flexible. To insert the thread, a small knot was tied at one end and a syringe was used to push the thread through the paths left by the syringes used for filling the liquid metal. The same uniaxial stretch test (5 cycles) was performed and the resistance response to strain is shown in Figure 16. The initial zero-strain resistance (2.627 Ω) was similar to the other gages with channels formed using the same method. However, unlike the response from the gages using copper wire, the resistance response using the thread was unstable. It is possible that the thread, especially with the small knot at the interface, was not making homogeneous contact with the liquid metal. This was unexpected, as previous research has shown better wetting between Galistan and conductive thread compared with Galistan and copper wire [24]. More likely, the unstable resistance was due to small amounts of liquid metal observed leaking from the fill port interface on one side as can be seen in Figure 15. The data backs this up as the changing resistance is more pronounced as the strain increases, thereby applying greater pressure on the gage.

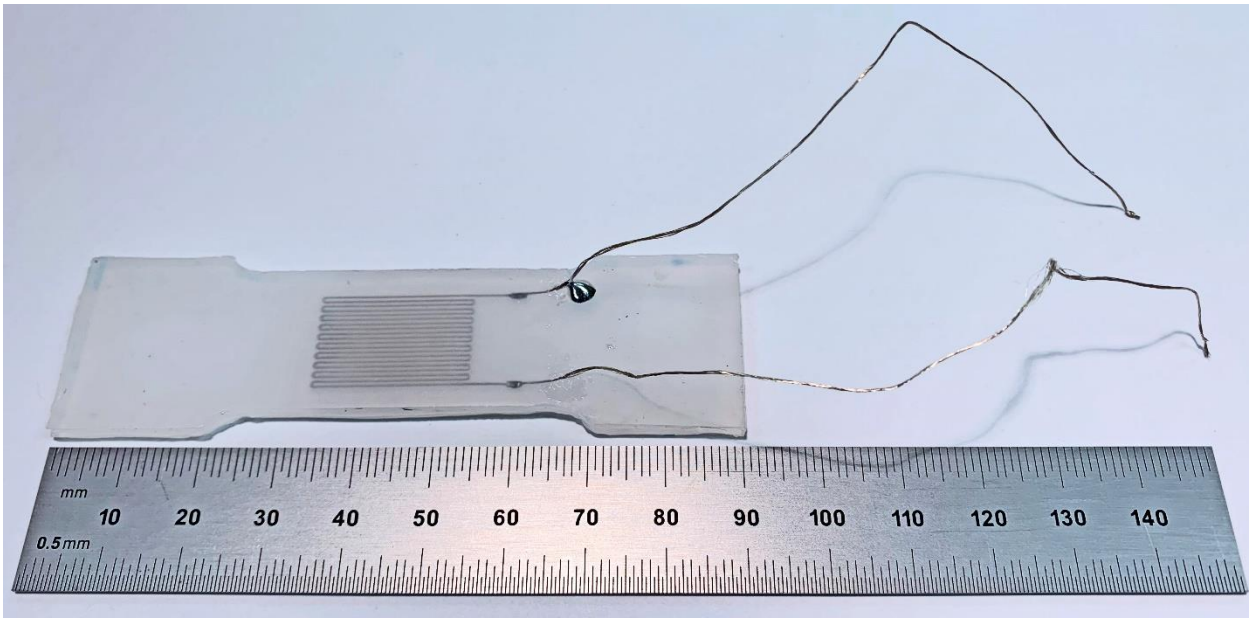

Figure 15: Photo of the gage assembled using Liberator 40 conductive thread as the electrical lead wire.

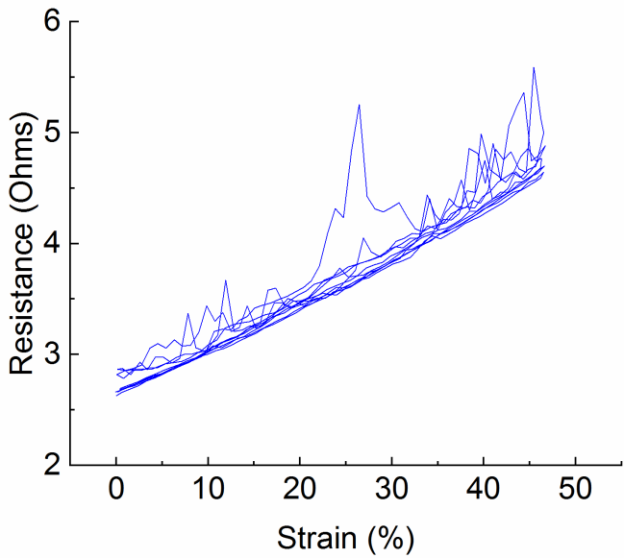

Figure 16: Resistance change with strain for a gage with channels formed using the tape on Si wafer fabrication technique and Liberator 40 conductive thread as the test leads.

Rosette Gage for Full 2D Strain Analysis

A soft rosette-style gage (Figure 17) made up of three stacked axial gages oriented at 45 degree relative orientations (0, 45, and 90 degrees) was assembled by casting using the tape on Si wafer method as shown in Figure 5e. The overall dimension of the square elastomer gage is 60 mm x 60 mm x 7.2 mm. Three layers of embedded channels and one solid layer were used and assembled by spin-coating in steps once the layer below was cured. The channels were filled with e-GaIn using the syringe method and 30 gage copper magnetic wire was inserted. The initial zero-strain resistances were 2.825, 2.793, and 2.164 Ω for the vertical (90 deg.), horizontal (0 deg.), and diagonal (45 deg.) gages, respectively. Cyclic uniaxial stretch testing was performed with the stretch direction aligned with the vertical (90 deg.) gage. A custom 3D printed clamp (orange device in Figure 17) was made to provide uniform stretch in the axial direction by interfacing between the testing machine grips and the square elastomer. The experimentally determined Poisson's ratio for this gage was 0.3905. While elastomer materials generally have Poisson's ratios near 0.5, other researchers [13] have obtained similar (0.39) experimentally found values. Figure 18 shows the gage sensitivities for both measured strains (axial and transverse). Since the gages have known calibrations based on their gage factors, these gages can work in visually-obscured gel materials to provide sufficient data for full 2D, independent strain component calculations. Although this gage was just an initial prototype, the data was linear and no hysteresis was observed. Future gages filled using an automated syringe method would enable reproducible initial zero-strain resistances that can further enhance the accuracy of these gages.

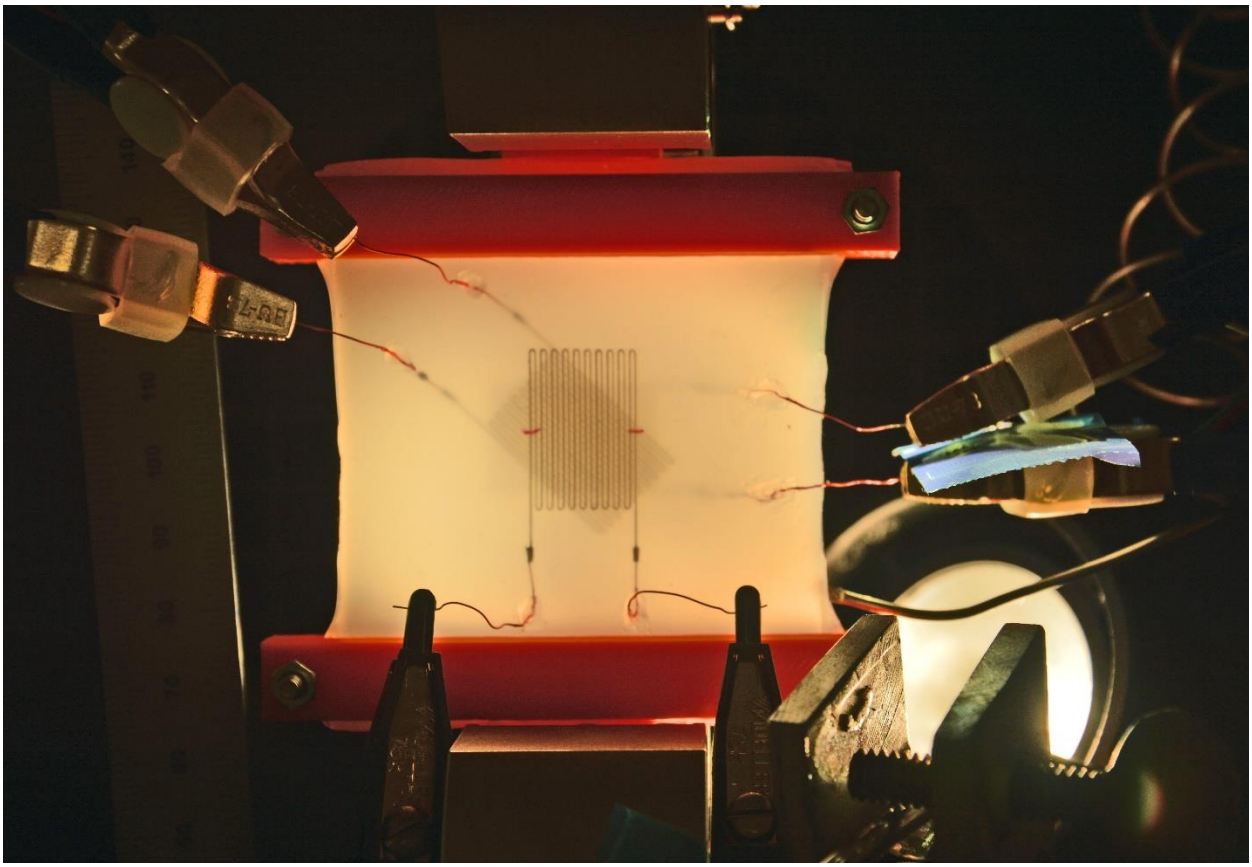

Figure 17: Backlit image showing the rosette-style gage with 3 sensors at 45° orientations.

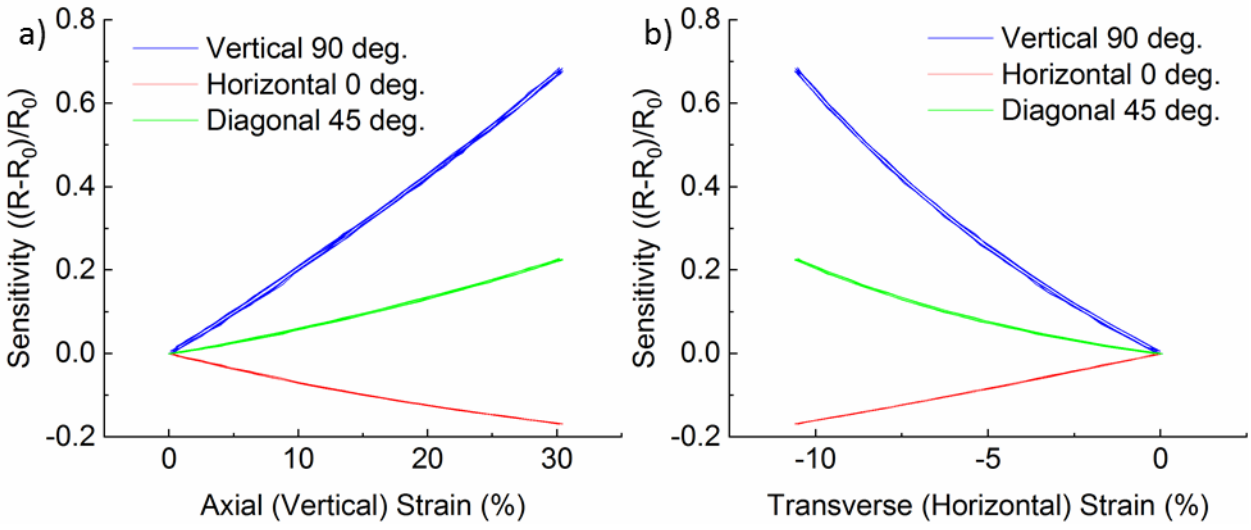

Figure 18: Sensitivity with respect to strain during uniaxial tensile stretching in the vertical direction with measured strain orientations in a) the axial vertical (aligned with 90 degree gage) direction and b) the transverse horizontal (aligned with the 0 degree gage) direction.

CHAPTER 4: CONCLUSIONS AND RECOMMENDATIONS

Deformation sensing of soft materials has been a challenge that only recently started receiving research attention for its applications in soft robotics and biomedical, wearable sensors. These applications benefit from the ability of soft sensors to provide positional feedback as well as multi-mode deformation quantifications. The motivation for this research, however, was to enable a greater understanding of the factors that lead to traumatic brain injury. To accomplish this, soft, impedance matched sensors that could measure normal and shear strains needed to be developed for use in bio-fidelic surrogate models. This research addressed two primary challenges to developing and implementing soft sensors: 1) how to measure normal and shear strains in visually obscured gel materials while ensuring impedance matching between the sensor and gel and 2) how to fabricate and calibrate the soft sensors without the need for high-end specialized equipment.

To address the first challenge, different conductive elements were examined for making the resistive strain element of the gage. Experimentation with ionic liquids, aqueous solutions, and liquid metals resulted in the decision to use eutectic-Gallium-Indium which is a room temperature liquid metal. The liquid metal has the benefit of being stable with electric current passage as well as non-reactive with the electrical lead wiring. For impedance matching, the sensor body was made of a platinum-cured silicone (EcoFlex 00-30) for its similar hardness and modulus properties as a typical bio-fidelic surrogate gel.

To overcome the second challenge, the original plan was to use a high-resolution additive manufacturing fused deposition 3D printer to make molds with serpentine channel elements. Due to an unfortunate acquisitions setback, three other fabrication techniques were attempted and characterized for their resolution, reproducibility, and accuracy: 1) 3D printing using selective laser sintering, 2) direct laser raster ablation on already cast and cured elastomer, and 3) laser vector cutting flash tape adhered to a Si wafer to generate the serpentine channels for casting with a mold. All three methods produced working gages that were similar in sensitivity when cyclically stretched. Direct laser rastering the gage channels would be the best method for complex channel geometries (such as those for pressure sensors). The laser cutting of flash tape on a Si wafer has previously not been reported in literature. This novel fabrication method provided the greatest reproducibility and highest resolution compared with the others tested. The custom electronics used in the assessment of these prototypes provided the resolution necessary to calculate the sensor’s gage factors (calibration factors).

Filling of the channel elements proved to cause the greatest error in reproducibility with different gages of near-identical channel areas having different zero-strain starting resistances caused by different volumes of liquid metal being injected. It is recommended that in future research, an automated syringe pump is utilized for exactness in filled volume.

Using conductive thread as the electrical test leads in this work resulted in a leaking of the liquid metal and thereby an instability in the resistance response, however it is believed the benefits of its use merit additional research. Using the flexible, light-weight thread does not diminish the

electrical response while it enables greater mobility of the gage and significantly reduces the impedance mismatch at the interface between the gage and electrical leads. Two methods are proposed for future gage assembly with conductive thread electrical leads: 1) use a canula to first insert the conductive thread before filling so a knot doesn't need to be tied or 2) apply the thread to the spin-coated, uncured layer before bonding with the layer with channels. This second method would have the additional benefit of enabling the thread to be placed in a serpentine pattern for increased ability to stretch without breaking.

It is believed that additional research in this area is warranted. Developing these soft sensor technologies can advance soft tissue damage research as well as many other relevant fields including soft robotics and aerospace. In researching these systems, it was noted that there is always a tradeoff between the sensitivity of the gage and the linearity and hysteresis of the response. The materials used in making the gages of this research provided a balance that should be used as a starting point. The fabrication methods used and developed could be used in future research even if the sensor matrix and element materials are altered for specific applications.

The stacked rosette-style gage assembled and tested in this work has provided the proof of concept necessary to support the ability of these gages to characterize three independent strain components in 2-dimensions. It is hoped that this research will be continued in the future to enable full characterization of 3-dimensional deformations in soft materials.

REFERENCES

[1] M. D. Dickey, "Stretchable and Soft Electronics using Liquid Metals," *Adv Mater,* vol. 29, no. 27, Jul 2017.

[2] K. Elgeneidy, G. Neumann, M. Jackson, and N. Lohse, "Directly Printable Flexible Strain Sensors for Bending and Contact Feedback of Soft Actuators," *Frontiers in Robotics and AI,* vol. 5, 2018.

[3] J. Sirohi and I. Chopra, "Fundamental Understanding of Piezoelectric Strain Sensors," *Journal of Intelligent Material Systems and Structures,* vol. 11, no. 4, pp. 246-257, 2016.

[4] T. Wang, Farajollahi, M., Choi, Y.S., Lin, I.T., Marshall, J.E., Thompson, N.M., Kar-Narayan, S., Madden, J.D.W., Smoukov, S.K., "Electroactive Polymers for Sensing," *Interface Focus,* vol. 6, 2016, Art. no. 20160026.

[5] P. Roberts, Damian, D., Shan, W., Lu, T., Majidi, C., "Soft-Matter Capacitive Sensor for Measuring Shear and Pressure Deformation," presented at the IEEE International Conference on Robotics and Automation (ICRA), Karlsruhe, Germany, 2013.

[6] A. Frutiger *et al.*, "Capacitive soft strain sensors via multicore-shell fiber printing," *Adv Mater,* vol. 27, no. 15, pp. 2440-6, Apr 17 2015.

[7] T. R. Filanc-Bowen, G. H. Kim, and Y. M. Shkel, "Novel sensor technology for shear and normal strain detection with generalized electrostriction," presented at the SENSORS, 2002.

[8] L. Viry *et al.*, "Flexible three-axial force sensor for soft and highly sensitive artificial touch," *Adv Mater,* vol. 26, no. 17, pp. 2659-64, 2614, May 2014.

[9] A. Fassler and C. Majidi, "Soft-matter capacitors and inductors for hyperelastic strain sensing and stretchable electronics," *Smart Materials and Structures,* vol. 22, no. 5, 2013.

[10] M. Amjadi, K.-U. Kyung, I. Park, and M. Sitti, "Stretchable, Skin-Mountable, and Wearable Strain Sensors and Their Potential Applications: A Review," *Advanced Functional Materials,* vol. 26, no. 11, pp. 1678-1698, 2016.

[11] J. T. Muth *et al.*, "Embedded 3D printing of strain sensors within highly stretchable elastomers," *Adv Mater,* vol. 26, no. 36, pp. 6307-12, Sep 2014.

[12] S. Z. Guo, K. Qiu, F. Meng, S. H. Park, and M. C. McAlpine, "3D Printed Stretchable Tactile Sensors," *Adv Mater,* vol. 29, no. 27, Jul 2017.

[13] J.-B. Chossat, Y.-L. Park, R. J. Wood, and V. Duchaine, "A Soft Strain Sensor Based on Ionic and Metal Liquids," *IEEE Sensors Journal,* vol. 13, no. 9, pp. 3405-3414, 2013.

[14] S. G. Yoon, B. J. Park, and S. T. Chang, "Highly sensitive microfluidic strain sensors with low hysteresis using a binary mixture of ionic liquid and ethylene glycol," (in English), *Sensors and Actuators a-Physical,* vol. 254, pp. 1-8, Feb 1 2017.

[15] Y. N. Cheung, Y. Zhu, C. H. Cheng, C. Chao, and W. W. F. Leung, "A novel fluidic strain sensor for large strain measurement," (in English), *Sensors and Actuators a-Physical,* vol. 147, no. 2, pp. 401-408, Oct 3 2008.

[16] R. J. W. Yigit Menguc, "Characterizing an elastomeric strain sensor at large strains and strain rates," in *Soft Robotics Workship at Robotics Sciencen and Systems*, 2014.

[17] Y. L. Park, C. Majidi, R. Kramer, P. Berard, and R. J. Wood, "Hyperelastic pressure sensing with a liquid-embedded elastomer," (in English), *Journal of Micromechanics and Microengineering,* vol. 20, no. 12, Dec 2010.

[18] D. M. Vogt, Y. L. Park, and R. J. Wood, "Design and Characterization of a Soft Multi-Axis Force Sensor Using Embedded Microfluidic Channels," (in English), *Ieee Sensors Journal,* vol. 13, no. 10, pp. 4056-4064, Oct 2013.

[19] J. C. Case, E. L. White, and R. K. Kramer, "Soft Material Characterization for Robotic Applications," *Soft Robotics,* vol. 2, no. 2, pp. 80-87, 2015.
[20] A. Fassler and C. Majidi, "3D structures of liquid-phase GaIn alloy embedded in PDMS with freeze casting," *Lab Chip,* vol. 13, no. 22, pp. 4442-50, Nov 21 2013.
[21] S.-H. Bae, Y. Lee, B. K. Sharma, H.-J. Lee, J.-H. Kim, and J.-H. Ahn, "Graphene-based transparent strain sensor," *Carbon,* vol. 51, pp. 236-242, 2013.
[22] P. Yong-Lae, C. Bor-Rong, and R. J. Wood, "Design and Fabrication of Soft Artificial Skin Using Embedded Microchannels and Liquid Conductors," *IEEE Sensors Journal,* vol. 12, no. 8, pp. 2711-2718, 2012.
[23] E. L. White, J. C. Case, and R. K. Kramer, "Multi-Element Strain Gauge Modules for Soft Sensory Skins," (in English), *Ieee Sensors Journal,* vol. 16, no. 8, pp. 2607-2616, Apr 15 2016.
[24] L. J. Teng, K. Jeronimo, T. Q. Wei, M. P. Nemitz, G. Lyu, and A. A. Stokes, "Integrating soft sensor systems using conductive thread," (in English), *Journal of Micromechanics and Microengineering,* vol. 28, no. 5, May 2018.

APPENDIX A: ELECTRONICS AND DATA AQUISITION

Unlike traditional metal strain gages that have standard initial resistances of 120 or 350 Ω and a known gage factor calibration, custom made soft strain sensors with a liquid metal sensing element have much lower initial resistances (< 10 Ω). The low resistances make the error due to test lead resistance and contact resistance amplified. The custom built breadboard that was designed an assembled for this project was able to both provide current and read the voltage change across the sensor by making gages with a 4-wire Kelvin configuration (shown in Figure 1). This configuration amplified the signal using a programmable digital gain and provided the desired readouts. The reason this system was not implemented for testing was that the many temporary connections via breadboard were accompanied with noise with any slight movement. This setup would, however, work well if a system-on-chip of this design was professionally fabricated.

Instead, the NI DAQ system was utilized, which provided high reliability and resolution of the signals. Kelvin clips were utilized that allowed the gages to be made with only two wire connections as the Kelvin clips provide current and read voltage separately. Figure 19 provides a wiring diagram of a NI SCB-68A breakout box. On the right side, the wiring was setup to provide current through the three gages in series and the voltage readout across the three gages was read in the analog in ports of A0-A2. The analog out of the Instron load signal was read into port A3 and the four analog out signals from the video extensometer (time and 3 strains) were read on ports A4-A7.

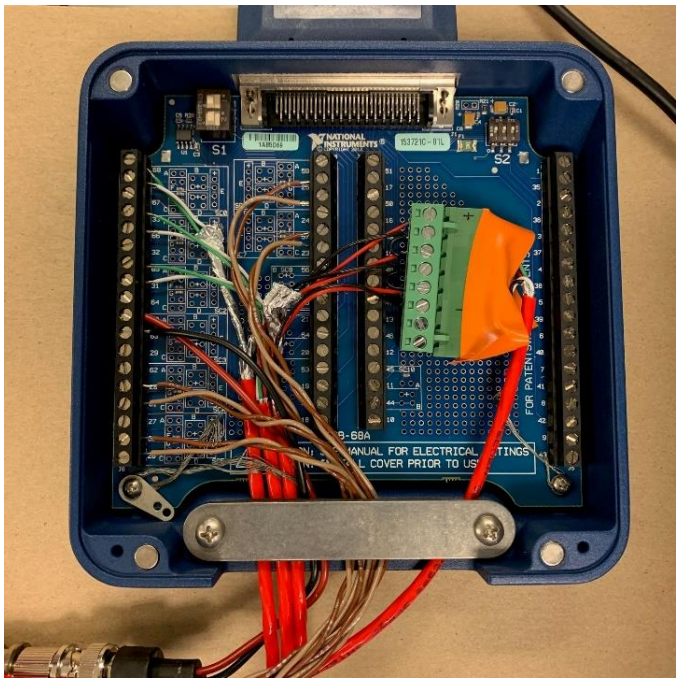

Figure 19: Image of the National Instruments SCB-68A breakout box with the wiring configured to provide current and read the voltage changes across 3 sensors in series. Additionally, the analog-out signals from the video extensomer were wired into ports A4-7 that were also converted to digital signals and recorded in Labview.

Figure 20 shows an overview of the triple-gage setup in the Instron test system. The three gages are wired in series with Kelvin clips that provide the current through one side and read the voltage on the other side of each clip. This is a zoomed-out image of what is shown in Figure 17.

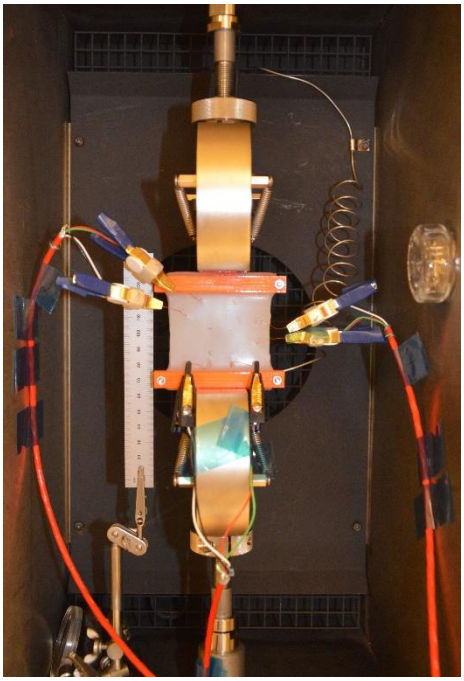

Figure 20: Image of the triple-gage in the Instron test system for cyclic stretch testing.

The video extensometer utilized a Mako G-503B monochrome CMOS camera (Allied Vision Technologies) with a varifocal 4-12 mm focal length video lens. The lens was set to a focal length of 4 mm and set at a working distance of 368 mm.

APPENDIX B: RESISTANCE-STRAIN PLOTS

The following plots show the resistance change with strain for the dogbone gages made using the three different channel fabrication techniques. The gages were strained from 0 to 50% for 5 cycles. The overlapping of the 5 cycles shows that no hysteresis was observed.

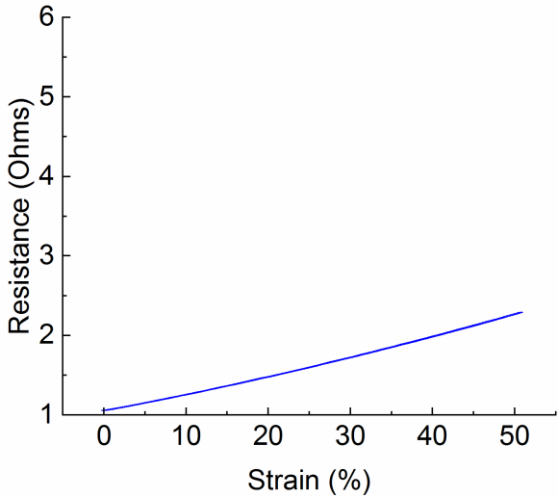

Figure 21: Resistance versus strain plot for gage: 3D printed mold – 1

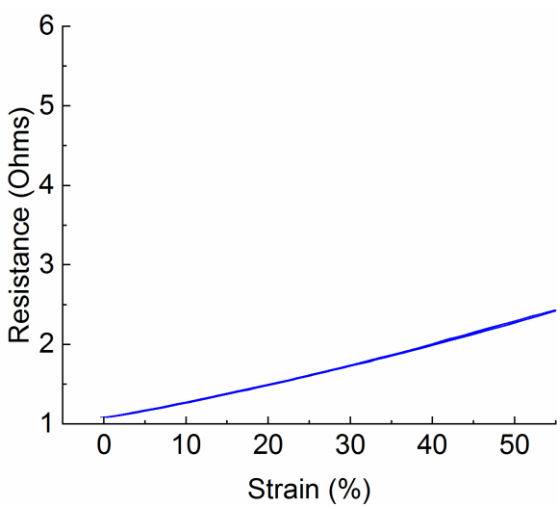

Figure 22: Resistance versus strain plot for gage: 3D printed mold – 2

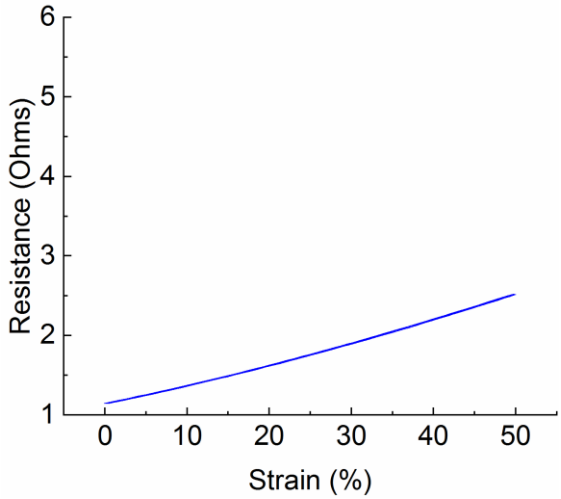

Figure 23: Resistance versus strain plot for gage: Direct laser raster – 1

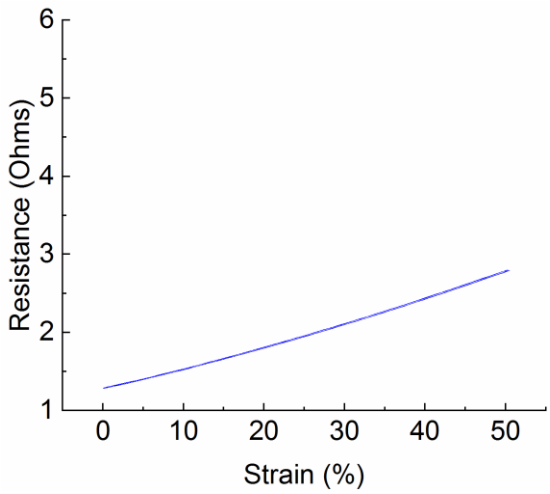

Figure 24: Resistance versus strain plot for gage: Direct laser raster – 2

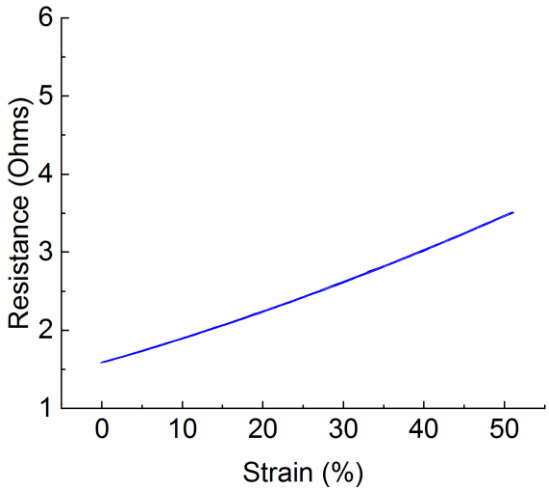

Figure 25: Resistance versus strain plot for gage: Direct laser raster - 3

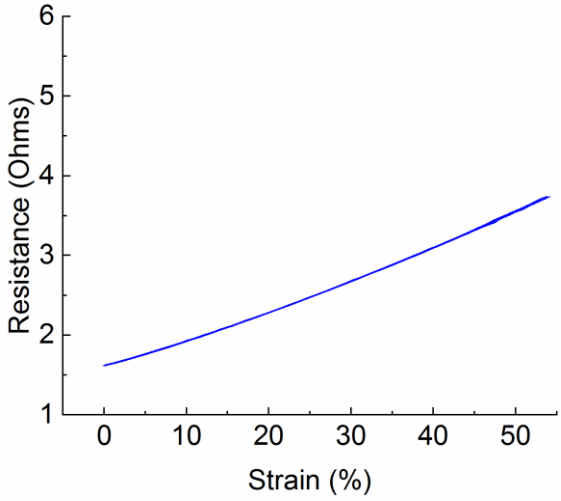

Figure 26: Resistance versus strain plot for gage: Tape on Si - 1

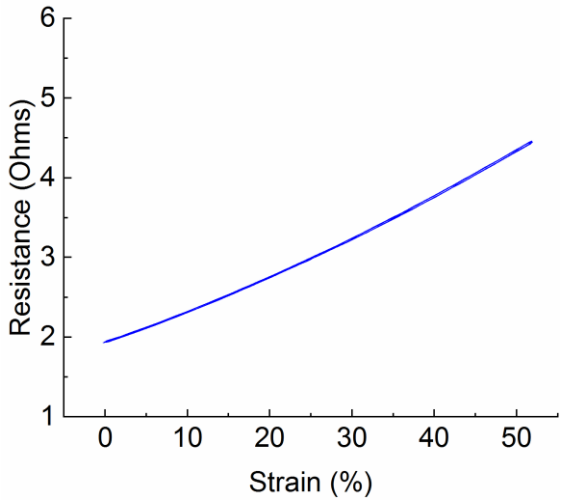

Figure 27: Resistance versus strain plot for gage: Tape on Si – 2

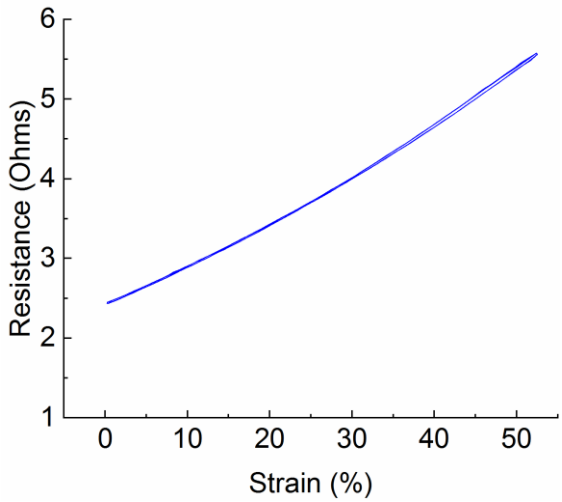

Figure 28: Resistance versus strain plot for gage: Tape on Si - 3